Iranian Journal of Catalysis 9(4), 2019, 281-292

IRANIAN JOURNAL OF CATALYSIS

Evaluation of sodium dodecyl sulfate effects; the response of modified carbon paste electrode with nickel oxide nanoparticles in the presence of methanol

Banafsheh Norouzi*, Mehdi Norouzi

Department of chemistry, Qaemshahr Branch, Islamic Azad University, Qaemshahr, Iran.

Received 23 July 2018; received in revised form 25 September 2018; accepted 5 October 2018

ABSTRACT

Synthesis of nickel oxide nanoparticles (NiO NPs) was carried out by *Marrubium astranicum* leaf extract. The average of particle sizes for NiO NPs was 40 nm. NiO NPs modified carbon paste electrodes in the absence (CPE/NiO NPs) and the presence of sodium dodecyl sulfate (CPE/NiO NPs/SDS) were examined for the electrocatalytic oxidation of methanol in alkaline solutions. The cyclic voltammograms of modified electrodes showed the redox behavior of Ni(III)/Ni(II) couple. However, the presence of SDS at the surface of the electrode increased the efficiency of the catalyst. The values of charge transfer coefficients (α) for the CPE/NiO NPs and CPE/NiO NPs/SDS in the presence of methanol were estimated at about 0.63 and 0.84. Finally, the electrocatalytic oxidation of methanol at the surface of the CPE/NiO NPs/SDS was studied in the optimum conditions (30 min for immersion time in SDS solution, 0.01 M for SDS concentration and 0.4 M for methanol concentration).

***Keywords**: Methanol, Electrocatalytic, Nickel oxide, Nanoparticle, Modified electrode.*

1. Introduction

Direct methanol fuel cells (DMFCs) can be used for various power applications and electric vehicles [1]. It has been considered safe compared to the H_2/air fuel cell. Their main advantage is the ease of transport of methanol, simple operation and stable liquid at environmental conditions [2-9]. The slow kinetics of methanol oxidation on the fuel cell's anode is one of the problems and it is not still solved [10]. Therefore, a highly efficient electrocatalyst is needed and the electrochemical oxidation of methanol at different modified electrodes has been receiving much attention [11-14].

Platinum and Pt-based electrocatalysts have usually been used as anodes in such DMFC [15-19] but these electrodes are costly, poisoning by products from oxidation and intermediates, and they have limited sources [20]. Many electrodes based on nickel can be used as an electrocatalyst for both anodic and cathodic reactions in organic synthesis and water electrolysis [21–24]. One of the very important uses of nickel as a catalyst is for the oxidation of alcohols. It is an effective and cheap catalyst. Several studies of the electro-oxidation of alcohols on Ni have been reported [2,25-28]. Also, applications of nickel nanoparticles as catalysts in fuel cell have been reported [29-31]. Properties of nanoparticles are getting more attractive when the size of the particles decreases. The research in these fields is still under progress to increase low cost efficiency.

Compared to metals, it is known that metal oxides have higher chemical stabilities in various media. NiO is a p-type semiconductor metal oxide which has been widely investigated for its application in energy storage devices such as Li-ion batteries, supercapacitors [32,33], anode material in electrochromic devices and supercapacitors [34,35], water remediation through photocatalysis [36], catalysis of chemical processes [37], and electrochemical sensing [38-40]. Recently, NiO nanoparticles have shown a good behavior toward electrooxidation of methanol [41-44].

The study of the methanol electro-oxidation in alkaline solutions has many advantages such as a wider selection of possible electrode materials [45], a better efficiency of the oxygen cathode [45], increased efficiency [46,47], negligible poisoning effects [48, 49], moreover the oxidation reactions of organic fuels exhibit almost

---

*Corresponding author.
E-mail address: norouz2020@yahoo.com (B. Norouzi)

no sensitivity to the surface structure in alkaline solutions [50].

On the other hand, surfactants (surface active agents) have important effects on electrode reactions such as more dissolution of organic compounds, control of electrochemical reactions, altering or enhancing of reaction rates, control of reaction pathways, improvements in the performance of batteries and fuel cells, inhibition of corrosion and promotion in electroplating techniques [51,52]. These molecules can give rise to adsorbed layers by varying thickness of monolayers, bilayers or multilayer of a very complex structure [53], thus affecting the rate of electrode reaction [54]. SDS is a synthetic organic compound with the formula of $CH_3(CH_2)_{11}SO_4Na$. It is an anionic surfactant which has a 12-carbon tail attached to a sulfate group.

Previously, we have used the dispersion of metallic ions on the modified carbon paste electrode by the construction of CPE/PINA(SDS)/Ni-Co [55] and CPE/PINA(SDS)/Ni-Pd [56] which can successfully catalyze the oxidation of methanol in an alkaline medium. Our literature survey indicates that there is no report as yet on the use of modified carbon paste electrode with NiO NPs in the presence of SDS for methanol electrooxidation. Thus, in present work, first, we synthesized NiO NPs with *Marrubium astranicum* leaf extract. Then, modification of the carbon paste electrode with NiO NPs was accomplished through introducing SDS at the surface of the electrode. Simplicity, low cost, and high stability are prominent properties of this electrode. Ultimately, this electrode is used for methanol electrooxidation.

2. Experimental

2.1. Reagents and materials

Nickel nitrate hexahydrate ($Ni\ (NO_3)_2.6H_2O$), sodium hydroxide, and ethanol were purchased from Fluka (Sydney, Australia) origin. Methanol and SDS were prepared from Merck (New Jersey, US). High viscosity paraffin (density 0.88 g cm^{-3}) from Fluka (Sydney, Australia) was used as the pasting liquid for CPE. Graphite powder (particle diameter 0.10 mm) from Merck (New Jersey, US) was used as the working electrode (WE) substrate. All other reagents were of analytical grade. Deionized water was used in the preparation of all aqueous solutions.

2.2. Apparatus

A gas chromatograph model Agilent-6890N equipped with the mass spectrometer and a split/splitless injector were used. HP-5 MS column (30 m×0.25 mm, film thickness: 0.5 μm) was used in the same operating conditions as above. Helium and nitrogen (99.999%) were used as a carrier and make-up gas, respectively. The flow rate of carrier gas was adjusted at 1 ml min^{-1}. The oven temperature was programmed as follows: 50 °C for 5 min, at 5 °C min^{-1} to 250 °C, 20 min held at 250 °C.

Phase identification, purity and crystallite size determination were carried out using XRD (Philips PW1730, Holand) at CuKα radiation, λ = 1.5406 Å, using the 2θ range of 10–80° with the step width of 0.05° and step time of 1 s.

The morphology and size of NiO NPs were characterized by a scanning electron microscopy (SEM, JSM-6610 LV FE).

Electrochemical experiments were conducted using a computer controlled potentiostat/galvanostat μ-Auto lab type III modular electrochemical system (Eco Chemie BV, Netherlands), driven with a general purpose electrochemical system (GPES) software (Nova). A CPE/NiO NPs/SDS was employed as a working electrode, an Ag|AgCl|KCl (3 M) as the reference electrode and a platinum wire as a counter electrode. All experiments were carried out at room temperature.

2.3. Preparation of plant extract

Marrubium astranicum leaves were collected from Kiasar city (Iran). These were dried in a laboratory oven at 50 °C and ground to powder form. 50 g of the powder was digested in 2000 mL ethanol and it was kept for 72 h, then filtered and stored. This was used as the extract for the synthesis of NiO NPs.

2.4. Preparation of NiONPs

For the synthesis of NiO NPs, aqueous nickel nitrate (250 mL, 0.1 M) was added to *Marrubium astranicum* extract (500 mL, 25 g L^{-1}) under vigorous stirring for 2 hours. The solution was kept overnight and then centrifuged. The precursor obtained was calcined in a furnace at 400 °C for 2 hours, this resulted in a black solid mass. It was analyzed by XRD. Fig. 1 shows how to prepare NiO NPs by use of reduced agents in *Marrubium astranicum* leaf extracts.

2.5. Surface modification of electrode

Carbon paste (CP) was prepared by grinding 0.67 g graphite powder and 0.33 g paraffin oil with a mortar and pestle and then by hand mixing to get a homogenous paste. A portion of prepared paste was packed into the end of a glass tube (internal radius: 1.0 mm) with a copper wire as an electrical contact. The surface of paste was smoothed on a piece of paper. This electrode was named CPE.

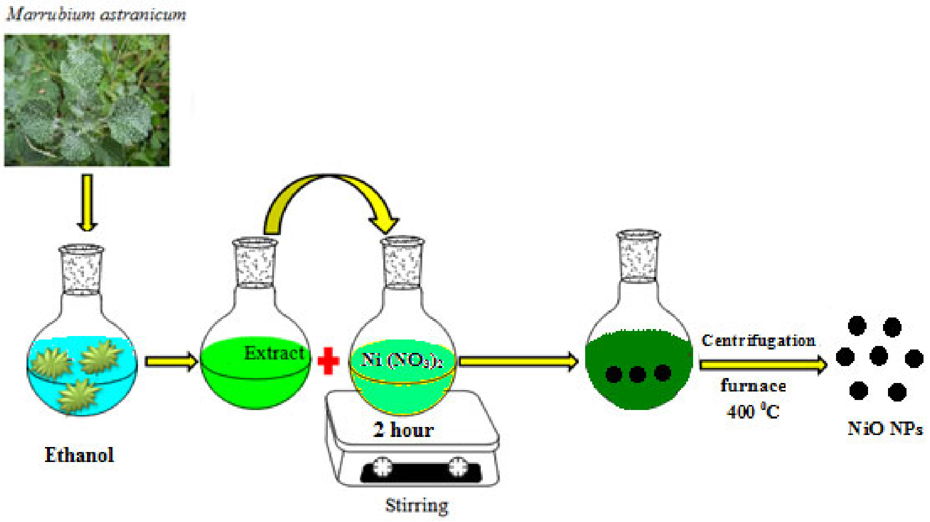

Fig. 1. Synthesis route for NiO NPs by *Marrubium astranicum* leaf extract.

Modified carbon paste electrode containing NiO NPs was obtained by homogeneously mixing of 0.067g NiO NPs and 0.603 g graphite powder and then 0.33 g paraffin oil was added drop-wise until a uniformly wet paste was obtained. A portion of prepared paste was packed into the end of a glass tube with a copper wire as an electrical contact. The surface of paste was smoothed on a piece of paper. This electrode was named CPE/NiO NPs. Then, the surface modification of the electrode was done by introducing SDS at the surface of the modified electrode. For this purpose, the solution of the 0.01 M SDS was prepared and the modified electrode was dipped in the solution of SDS. Electrode remained dip in the solution along magnetic stirring for 30 min. Then, modified electrodes were washed with distilled water. At the beginning of the experiment, the CPE/NiO NPs/SDS was immersed in 0.1 M NaOH solution and the potentials were cycled between 0.1 and 0.8 V vs. Ag|AgCl|KCl (3 M) at v=50 mV s^{-1} until a reproducible cyclic voltammogram (CV) was attained. Fig. 2 shows the procedure for the construction of the CPE/NiO NPs/SDS.

3. Results and Discussion

3.1. Analysis of plant extract

The gas chromatography (GC)–mass spectroscopy (MS) analysis of dried plant extract showed that the plant extract contains 22 different compounds. The analysis revealed that the major component of the extract is Marrubiin. It is a widely known diterpenoid lactone that constitutes the bitter principle of the horehound and many other medicinal plants of the family Lamiaceae [57]. MS analysis of these compounds showed the presence of terpenes (70%) and fatty acids and its ester (4.71%). Also, CHNS analysis of plant extract showed the presence of carbon (49.9%), hydrogen (1.64%), nitrogen (1.55%), sulfur (7.56%), metals and oxygen (rest).

Total Phenolic Content (TPC) of the extract was determined by the Folin–Ciocalteu method [58,59]. The TPC was calculated from the calibration curve (Absorbance vs. different concentration of a gallic acid standard solution), and the results were expressed as mg of gallic acid equivalent per g of extract. Based on the calibration curve, TPC of the extract was equal to 33.3 mg g^{-1}. These results showed that the presence of reducing agents such as TPC in *Marrubium astranicum* leaf extract is suitable for synthesizing NiO NPs.

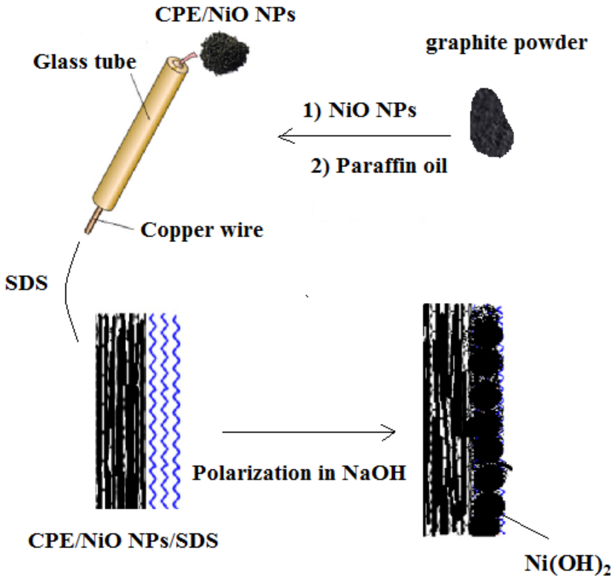

Fig. 2. Schematic procedure for construction of the CPE/NiO NPs/SDS.

3.2. Identification of NiO NPs

3.2.1. XRD Analyses

Fig. 3 depicts the XRD patterns of the sample with a mole ratio of 1:2 nickel nitrate solution to extract. The XRD data are very well matched with the hexagonal phase NiO nanoparticles which (Bunsenite structure) are found in the lattice planes (hkl) of (111), (002), (022) and (113) at the 2θ values of 37.3, 43.42, 63.00, and 75.63 degrees, respectively by their comparison with the data from JCPDS card No. 98-000-8167 [60]. The crystallite size of the NiO NPs was calculated using the Scherrer's equation [61,62]:

$$d = k\lambda/\beta\cos\theta \qquad \textbf{(1)}$$

Where k is a constant (ca. 0.9) [63]; λ is the X-ray wavelength used in XRD (1.5418 A°); θ is the Bragg angle; β is the pure diffraction broadening of a peak at half-height, this broadening is due to the crystallite dimensions. The average crystallite size of the NiO NPs is ca. 40 nm.

3.2.2. SEM Images

Fig. 4 shows SEM image of the synthesized NiO NPs of *Marrubium astranicum* leaves. It was very useful for determination of the size and morphology of the obtained crystals. The results showed that these nanoparticles are generally semi-spherical in shape with some degree of aggregation taking place. Also, the particle size distributions were obtained by image analysis (Fig. 4B). Based on this figure, the most particle size is about 40 nm. This result showed that the average particle size calculated with XRD is consistent with the SEM results.

3.3. Electrochemical characterization

3.3.1. Electrochemical behavior of modified electrode

Fig. 5 shows the polarization behavior of the modified electrodes with NiO NPs in the absence and presence of SDS using a cyclic voltammetry technique in the potential range of 0.2–0.8 V with a potential sweep rate of 50 mV s^{-1}. This technique allows the oxide film formation to be in parallel to inspecting the electrochemical reactivity of the surface. As can be seen in this figure, the anodic and cathodic currents for both modified electrodes grow with the number of potential scans, indicating the enrichment of the electroactive species Ni (II) and Ni (III) in the surface.

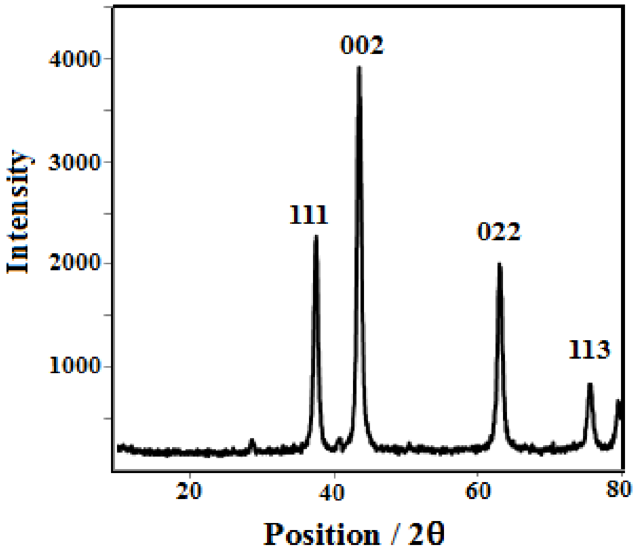

Fig. 3. XRD patterns of the NiO NPs produced by *Marrubium astranicum* extract.

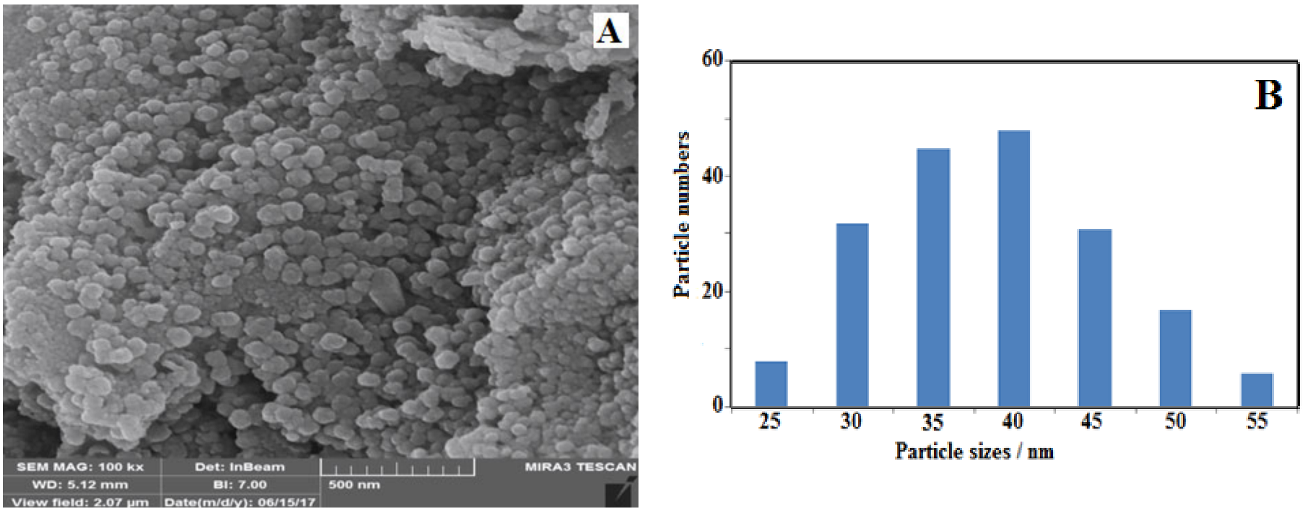

Fig. 4. SEM images of NiO NPs produced by *Marrubium astranicum* extract (A) Curve of particle size distribution of NiO NPs (B).

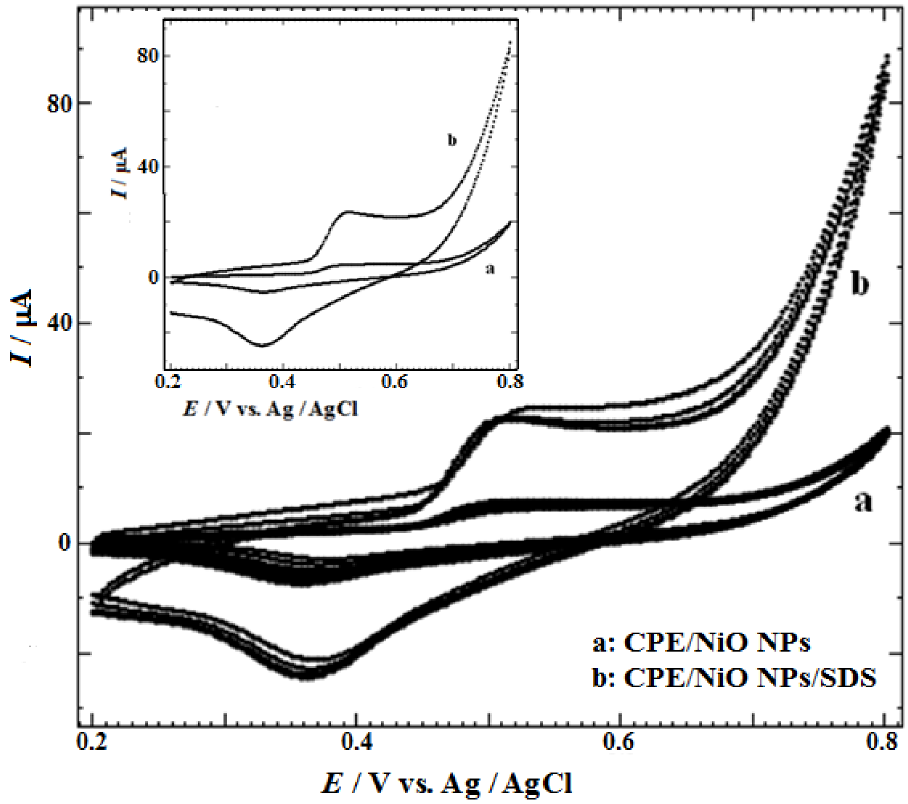

Fig. 5. Cyclic polarization behavior of (a) CPE/NiO NPs and (b) CPE/NiO NPs/SDS in 0.1 M NaOH (pH=13) with consecutive potential scans (n=5), Inset: Electrochemical responses of (*a*) CPE/NiO NPs and (*b*) CPE/NiO NPs/SDS after anodic polarization in 0.1 M NaOH solution (pH=13), υ =50 mVs^{-1}

Polarization results in a stationary state. The redox process of these modified electrodes in alkaline solution is expressed as [64]:

$$Ni(OH)_2 + OH^- \rightleftharpoons NiOOH + H_2O + e^- \qquad (2)$$

Also, the redox current in the presence of SDS is considerably higher than in the absence of it (Insert of Figure 5). This observation reflects that the effective active surface of the modified electrode is bigger in the presence of SDS. It shows that, in the presence of SDS, more nickel ions may easily reach the electrode surface and produce the more effective active surface. It has been seen a pair of well-defined peaks with a half-wave potential of about 430 mV vs. Ag|AgCl|KCl (3 M) for both modified electrodes. The peak-to-peak potential separation at v=50 mV s^{-1} is about 150 mV. The anodic peak current is proportional to the v (potential scan rate) at values from 5 to 100 mV s^{-1} (Figure not shown). The linear relationship between peak current and v indicates a surface-controlled process. This can be obtained from the slope of this line and using equation [65]:

$$I_p = n^2F^2vA\tau^*/4RT \qquad (3)$$

where I_p, A, and τ^* are peak current, electrode surface area and surface coverage of the redox species, respectively. The total surface coverage of the immobilized active substance at the surface of CPE/NiO NPs and CPE/NiO NPs/SDS is calculated about 3.86 × 10^{-9} and 8.69×10^{-9} mol NiO cm^{-2} (The slopes of I vs. υ were obtained to be 0.109 and 0.245 for modified electrodes, respectively.

3.3.2. Electrochemical behavior of the modified electrode in the presence of methanol

Fig. 6 shows the electrochemical behavior of methanol at the surface of CPE and CPE/SDS by cyclic voltammetric experiments in 0.1 M NaOH. No anodic and cathodic peaks were observed at the surface of CPE and CPE/SDS in the presence of methanol and in the investigated potential range (−0.2 to +1.2 V) because of slow electron transfer of methanol at the surface of them.

The electrochemical response of CPE/NiO NPs and CPE/NiO NPs/SDS has been shown in 0.1 M NaOH solution and in the presence of 0.1 M methanol (Fig. 7). Increasing the anodic peak current and decreasing the cathodic peak during the reverse scan are observed upon methanol addition to the electrolyte solution. The Ni (OH)$_2$ layer at the electrode surface acts as a catalyst for methanol oxidation.

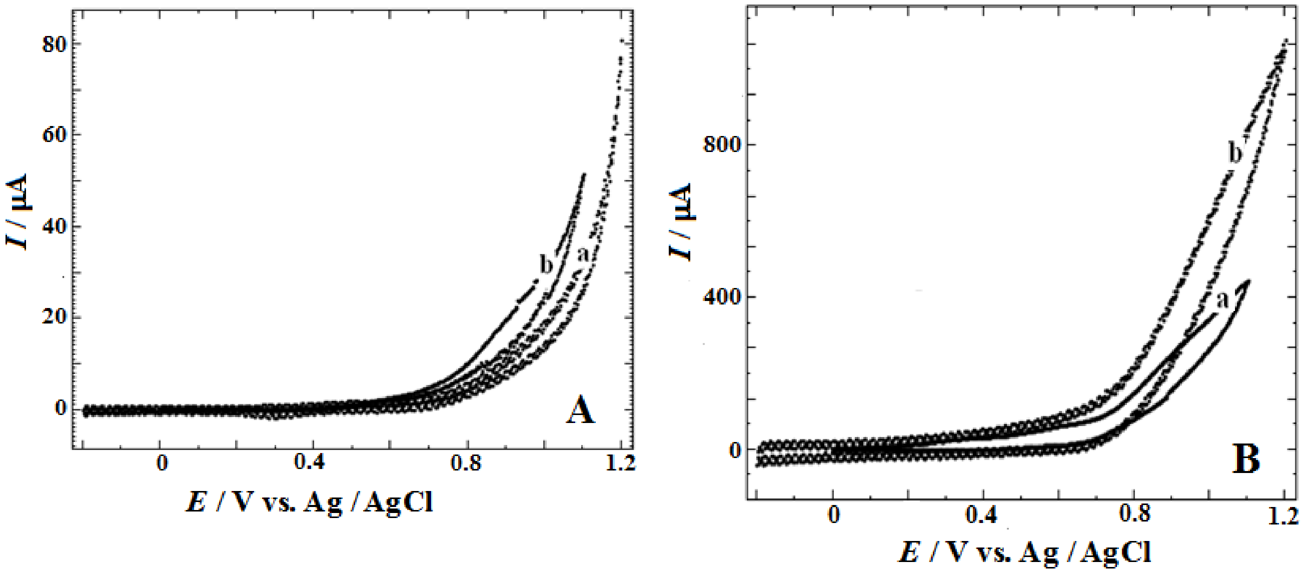

Fig. 6. Electrochemical responses of (A) CPE and (B) CPE/SDS in 0.1M NaOH solution (pH=13) with υ =20 mV s^{-1} in the (a) absence and (b) the presence of 0.10 M methanol, υ =20 mV s^{-1}.

The comparison of curves in the presence and absence of methanol is shown in Fig. 7C. As can be seen in this figure, the peak current of methanol oxidation at the surface of CPE/NiO NPs/SDS is about 1.5-fold greater than that at the CPE/NiO NPs. These observations can explain clearly the role of the SDS on the enhancement of the electrocatalytic oxidation currents of methanol. It seems that the main and plausible reason for such enhancement is the effective presence of nickel ions in the presence of SDS at the surface of CPE/NiO NPs/SDS which provides the facile arrival of methanol on nickel catalytic centers. Taking into account all these observations and also available literatures [28,30,55,66] the electrocatalytic oxidation mechanism (EC') of methanol at these modified electrodes may be described by:

$$Ni(OH)_2 + OH^- \rightleftarrows NiOOH + H_2O + e^- \qquad \textbf{(4)}\ E$$

$$NiOOH + Methanol \longrightarrow Ni(OH)_2 + products \qquad \textbf{(5)}\ C'$$

Fig. 7 depicted the plots of log I vs. E (Tafel plot) for the oxidation of 0.1 M of methanol at the surface of CPE/NiO NPs and CPE/NiO NPs/SDS at a scan rate of 5 mV s^{-1}. The rising part of the current-voltage of curve *b* on the voltammogram is affected by electron transfer kinetics between the modified electrode and methanol. The Tafel equation for anodic reactions is shown below [65]:

$$\log I = \log I_0 + (1-\alpha)\, nFE/\, 2.303RT \qquad \textbf{(6)}$$

where α is the transfer coefficient, I_0 is the exchange current, n is the number of electrons involved in the rate-determining step, F is the Faraday constant, R is the molar gas constant, and T is temperature. The Tafel slope for the CPE/NiO NPs and CPE/NiO NPs/SDS is equal to $n(1-\alpha)F/2.303\, RT$ which comes up to 6.26 and 2.75 V decade^{-1}, this indicates that charge transfer coefficients (α) for mediated electrooxidation of methanol are about 0.63 and 0.84, respectively. To the point where the overpotential equals zero, the exchange current can be calculated by extrapolating the Tafel lines. The exchange currents for the CPE/NiO NPs and CPE/NiO NPs/SDS catalysts are 7.7 × 10^{-6} and 8.5 × 10^{-4} mA, respectively. These results indicate that the CPE/NiO NPs/SDS electrocatalyst is more efficient than the CPE/NiO NPs electrocatalysts. The CPE/NiO NPs/SDS catalyst yielded a higher exchange current and charge transfer coefficient compared with the other catalysts; this may be related to the enhanced electrocatalytic activity in the methanol oxidation reaction.

3.4. Effect of different parameters on the response of modified electrode

3.4.1. The effect of immersion time in SDS solution

The electrocatalytic oxidation peak currents increased gradually when immersion times in SDS solution increased up to a maximum at 30 min. So, 30 min was chosen as the optimum time, which indicated that the saturated accumulation on the CPE/NiO NPs/SDS had been achieved (Fig. 8). It is well established that surfactants can be adsorbed on modified surfaces to form surfactant films [67]. The increasing sensitivity with the immersion time can also be rationalized by the increasing absorbance of SDS on electrode surface and increased presence of nickel ions on the surface of electrode.

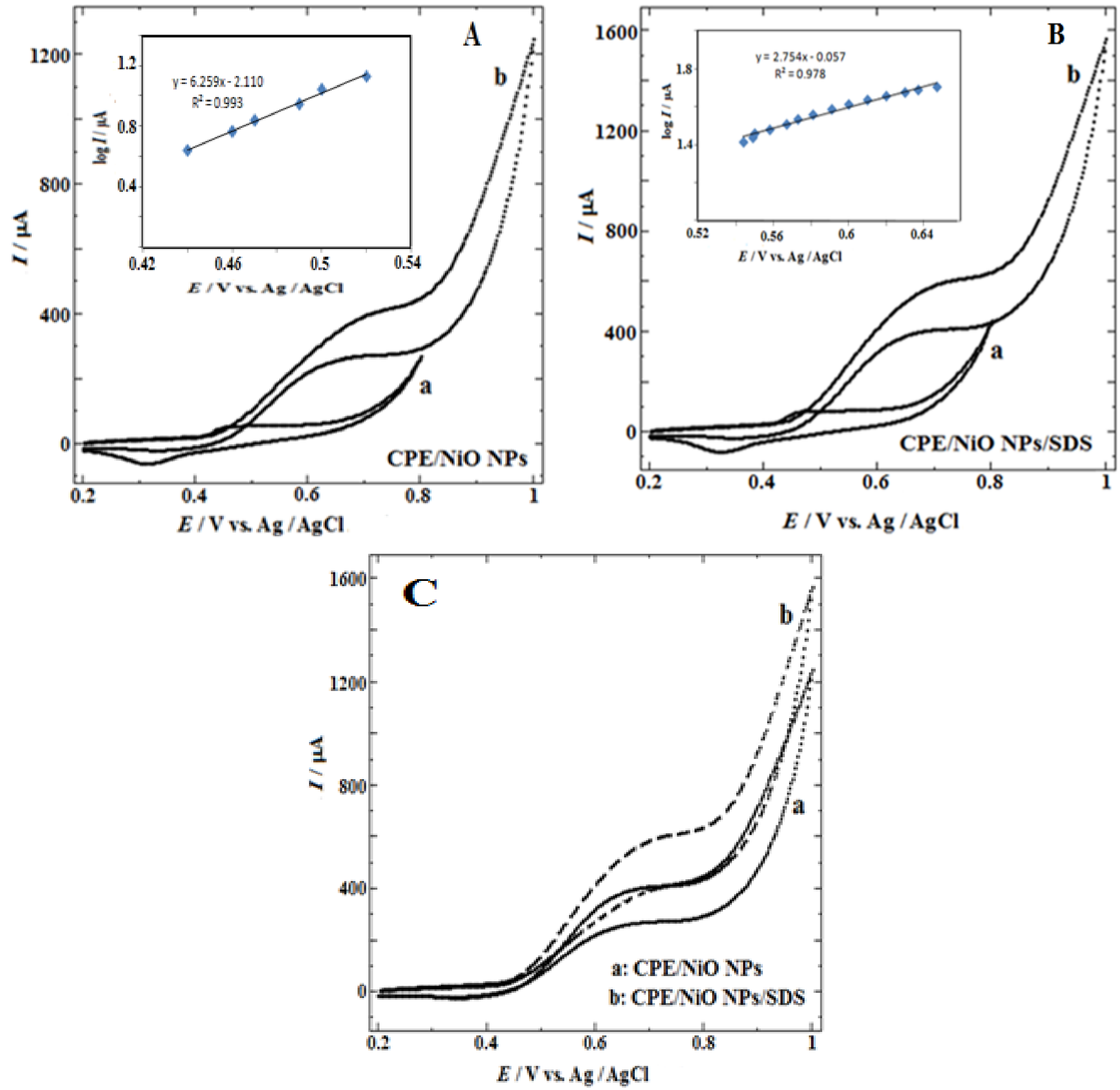

Fig. 7. Electrochemical responses of (A) CPE/NiO NPs and (B) CPE/NiO NPs/SDS in 0.1 M NaOH solution (pH=13) with υ =20 mV s^{-1} to: (a) 0.0 M, (b) 0.10 M methanol, (C) comparsion response of modified electrodes in the presence of methanol. Inset: Tafel plot derived from the rising part of the curve b for CPE/NiO NPs and CPE/NiO NPs/SDS.

3.4.2. The effect of SDS concentration

Surfactants play a very important role in electrode reactions, providing the specific orientation of the molecules at the electrode interface [68]. The influence of different concentrations of SDS (0.005, 0.01 and 0.05 M) on the electrocatalytic oxidation of methanol was investigated and the corresponding results are shown in Fig. 9. The increase of SDS concentration increases the anodic current apparently. The highest anodic peak current was considered as an optimum concentration. Therefore, we used a concentration of 0.01 M SDS to prepare CPE/NiO NPs/SDS. This concentration is close to the value of 0.0082 M for critical micelle concentration (CMC) of SDS at 25°C. At low SDS concentrations, the surface concentrations of nickel ions at the surface of modified electrode are low and the interactions between nickel ions and methanol are weak. When the SDS concentration is near about CMC, it is convinced that SDS may form a compact monolayer on the electrode surface and the density of this monolayer increases with SDS concentration.

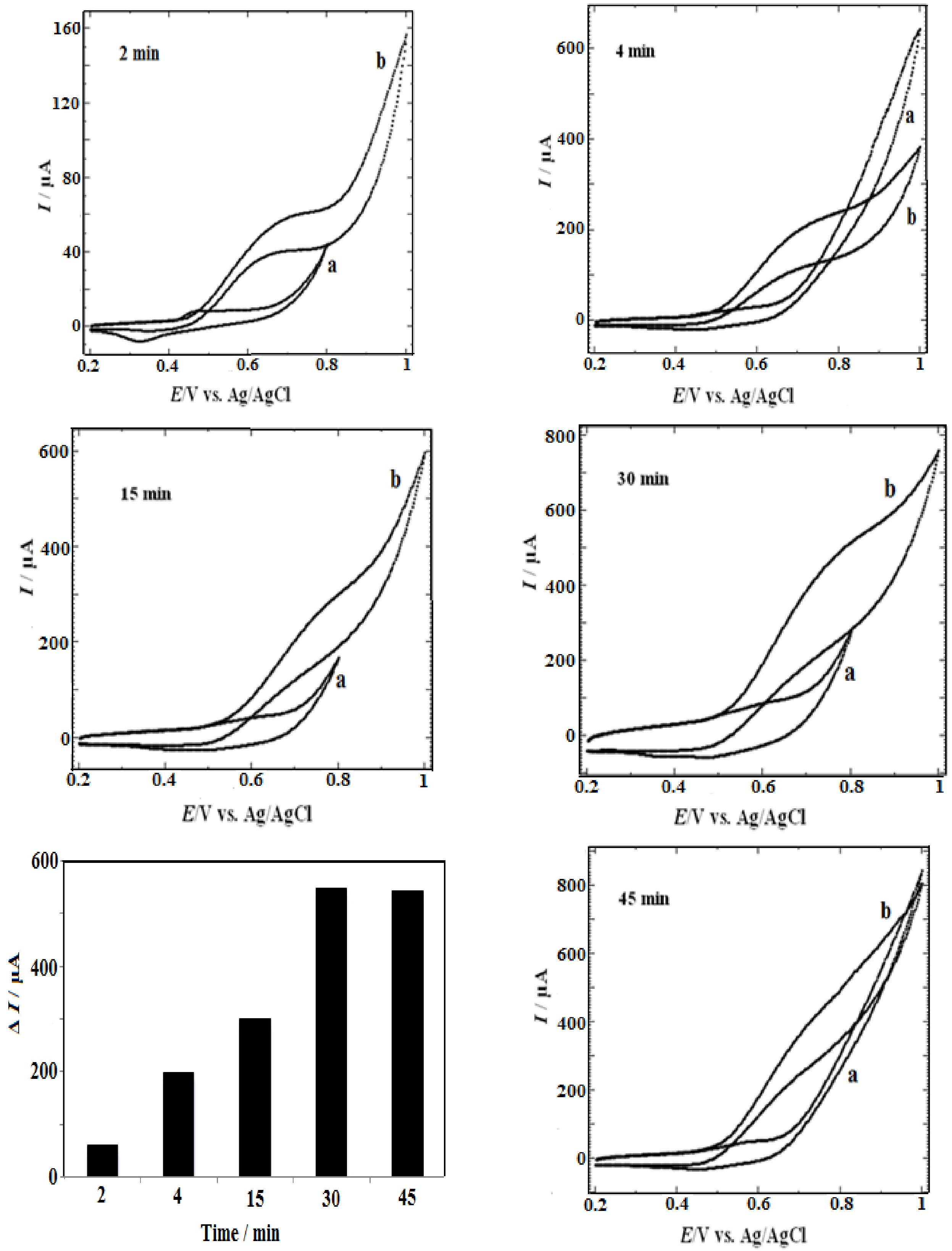

Fig. 8. Electrochemical responses in 0.1 M NaOH solution (pH=13) in the presence of 0.10 M methanol at *v*=20 mV s^{-1} for CPE/NiO NPs/SDS prepared in various immersion times in SDS solution in the modification steps. Inset: Variation of anodic peak currents with immersion times in SDS solution (SDS concentration=0.01 M).

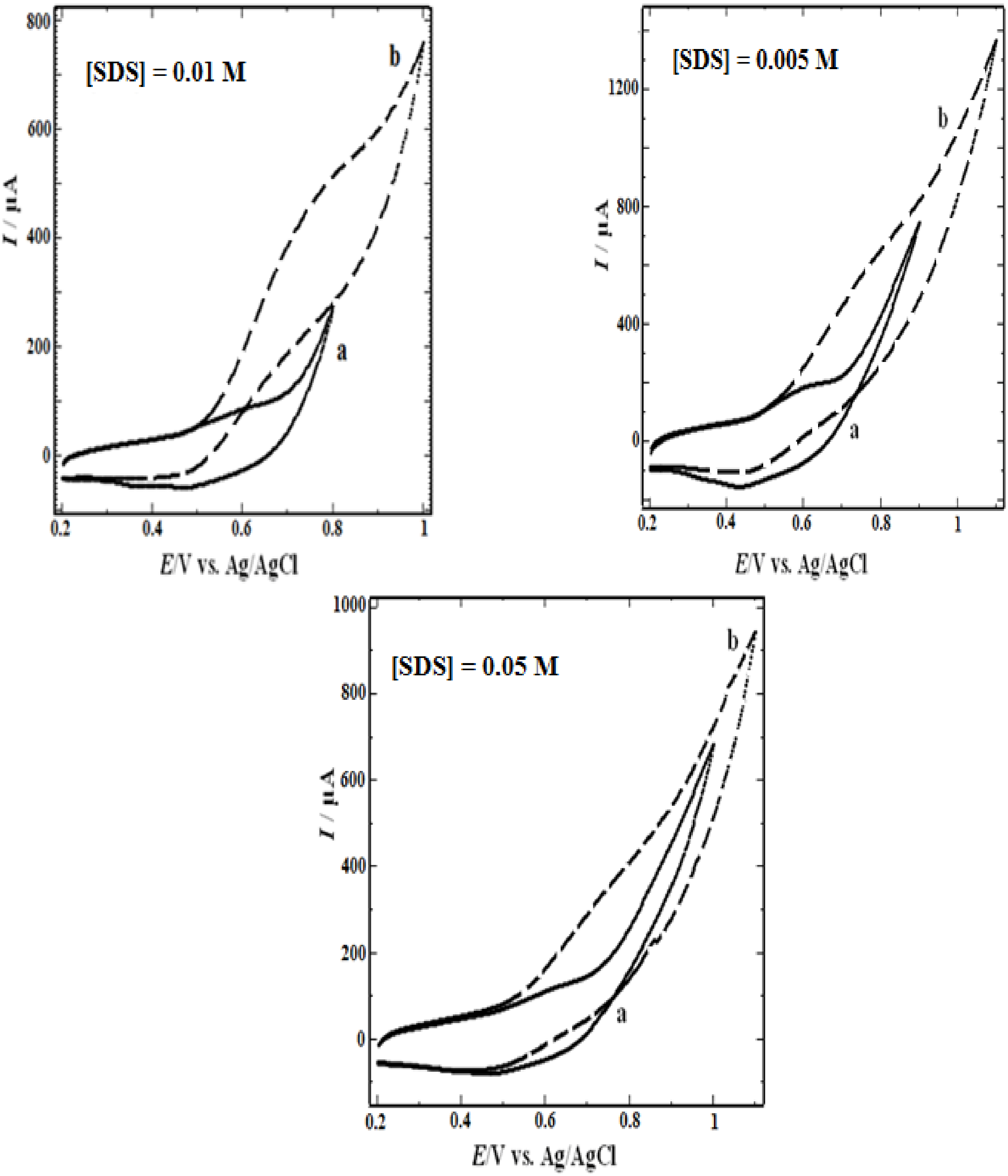

Fig. 9. Electrochemical responses in 0.1 M NaOH solution (pH=13) in the presence of 0.10 M methanol at *v*=20 mV s^{-1} for CPE/NiO NPs/SDS prepared in various concentrations of SDS solution in the modification steps. Inset: Variation of anodic peak currents with SDS concentration (immersion time in SDS solution =30 min).

At SDS concentrations greater than the CMC and when sufficient surfactant is present, the sorbed surfactant molecules primarily form a bilayer on the modified CPE surfaces. The surface concentration of nickel ions is very high and the electrostatic repulsion between them may result in the low peak current [69]. Fig. 10 represents the schematic description of the modified electrode.

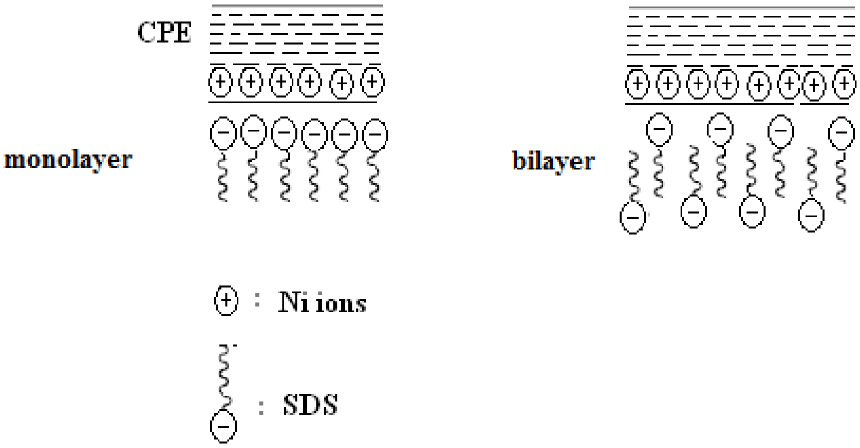

Fig. 10. Schematic representation for the CPE/NiO NPs/SDS.

3.4.3. The effect of methanol concentration

Fig. 11 shows the response of CPE/NiO NPs/SDS in the presence of several concentrations of methanol. It can be seen that the anodic peak current increases when the methanol concentration increases and reaches the steady state at higher concentrations. We assume this effect may be due to the saturation of active sites and/or poisoning the electrode surface with adsorbed intermediates. Thus, a concentration value of 0.4 M represents a critical concentration after which the adsorption of the oxidation products at the electrode surface causes the hindrance of further oxidation. Thus, a concentration value of 0.4 M is an optimum concentration with a higher current density [64].

3.5. Electrode stability, repeatability and reproducibility

It is obvious that the CPE/NiO NPs/SDS exhibits a good stability toward methanol oxidation. The stability of the modified electrode has been checked by measuring its response to methanol oxidation after 3 weeks of storage in the laboratory atmosphere condition. The electrode response to electrocatalytic oxidation of methanol retains 92% of the initial value. To investigate the repeatability of electrode, the CPE/NiO NPs/SDS was applied to the 5 parallel determinations of 0.1 M methanol and the relative standard deviation (RSD) was calculated as 3.2%. Further, under the same and independent conditions, it was found that the electrocatalytic oxidation currents of 0.1 M methanol almost remained the same by five with CPE/NiO NPs/SDS a RSD of 4%, indicating a high reproducibility.

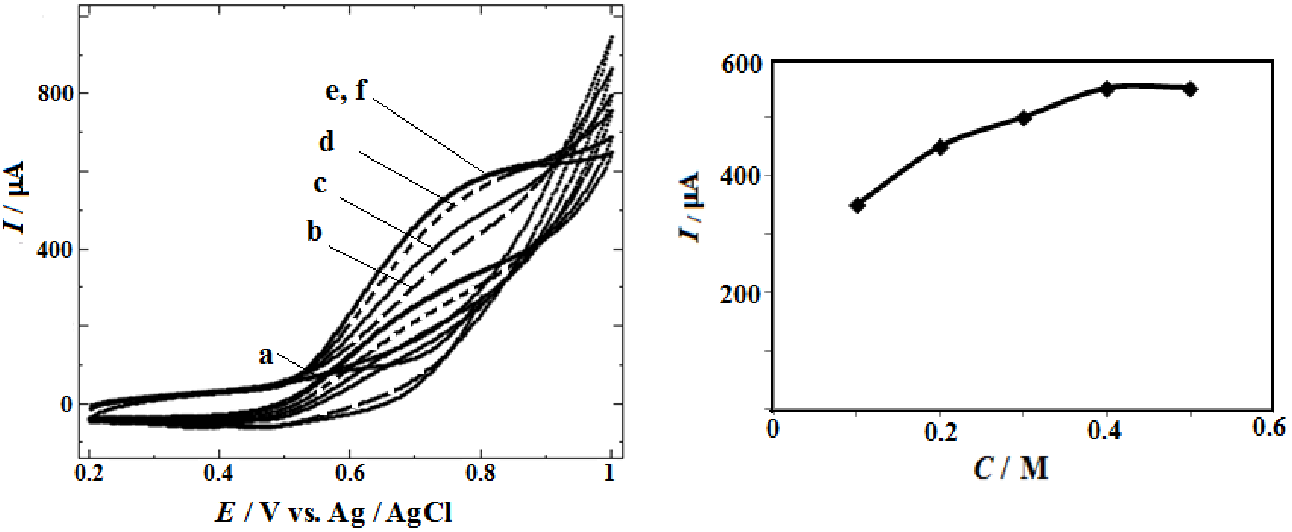

Fig. 11. Cyclic voltammograms of CPE/NiO NPs/SDS in 0.1 M NaOH solution (pH=13) with different concentrations of methanol *a* 0, *b* 0.1, *c* 0.2, *d* 0.3, *e* 0.4, and *f* 0.5 M, $v = 20$ mV s^{-1}. Inset: Plot of I_{pa} vs. methanol concentration.

4. Conclusions

In this work, CPE/NiO NPs/SDS was prepared by a simple method. NiO NPs have been successfully synthesized through one-step and cost-effective phytofabrication using nickel nitrate and leaf extract of *Marrubium astranicum*. This modified electrode showed good electrocatalytic activity for the oxidation of methanol. Addition of SDS leads to a higher increase in the electrocatalytic oxidation current of methanol than that in the absence of SDS. In comparison with some other previous works, it seems clear that CPE/NiO NPs/SDS in the modified electrode can act as a comparable catalyst in methanol oxidation (Table 1). The values of current density and anodic peak potential of methanol at the surface of this modified electrode are comparable with those obtained using other modified electrodes. Besides, the surface modification of the electrode is very simple and reproducible compared to other modified electrodes.

References

[1] J. Larminie, A. Dicks, Fuel Cell Systems Explained, Wiley, New York, 2000.

[2] I. Danaee, M. Jafarian, F. Forouzandeh, F. Gobal, M.G. Mahjani, Int. J. Hydrogen Energy 33 (2008) 4367–4376.

[3] B. Habibi, S. Ghaderi, J. Iran. Chem. Soc. 14 (2017) 1633–1642.

[4] R.A. Mirzaie, F. Hamedi, Iran. J. Catal. 5 (2015) 275-283.

[5] M.H. Nobahari, A. Nozad Golikand, M. Bagherzadeh, Iran. J. Catal. 7 (2017) 327-335.

[6] M.S. Tohidi, A. Nezamzadeh-Ejhieh, Inter. J. Hydrogen Energy 41 (2016) 8881-8892.

[7] A. Samson Nesaraj, M. Kumar, I. Arul Raj, I. Radhakrishna, R. Pattabiraman, J. Iran. Chem. Soc. 4 (2007) 89-106.

[8] A.S. Nesaraj, I.A. Raj, R. Pattabiraman, J. Iran. Chem. Soc. 7 (2010) 564-584.

[9] B.M. Daas, S. Ghosh, J. Iran. Chem. Soc. 15 (2018) 987–996.

[10] T.D. Jarvis, E.M. Stuve, In: J. Lipkowski, P. Ross, (Ed.), Electrocatalysis, Wiley-VCH, 1998.

[11] Z. Mousavi, A. Benvidi, S. Jahanbani, M. Mazloum-Ardakani, R. Vafazadeh, H.R. Zare, Electroanalysis 28 (2016) 2985-2992.

[12] K.L. Nagashree, M.F. Ahmed, J. Solid State Electrochem. 14 (2010) 2307–2320.

[13] H. Razmi, E. Habibi, H. Heidari, Electrochim. Acta 53 (2008) 8178-8185.

[14] J.B. Raoof, N. Azizi, R. Ojani, S. Ghodrati, M. Abrishamkar, F. Chekin, Int. J. Hydrogen Energy 36 (2011) 13295-13300.

[15] A.V. Tripkovic, K.D. Popovic, J.D. Lovic, V.M. Jovanovic, A. Kowal, J. Electroanal. Chem. 572 (2004) 119–128.

[16] A.V. Tripkovic, K.D. Popovic, B.N. Grgur, B. Blizanac, P.N. Ross, N.M. Markovic, Electrochim. Acta 47 (2002) 3707-3714.

[17] Y.G. Zhou, J.J. Chen, F. Wang, Z.H. Sheng, X.H. Xia, Chem. Commun. 46 (2010) 5951-5953.

[18] F. Kadirgan, S. Beyhan, T. Atilan, Int. J. Hydrogen Energy 34 (2009) 4312-4320.

[19] Y. Lou, M.M. Maye, L. Han, J. Luo, C.J. Zhong, Chem. Commun. 5 (2001) 473-474.

[20] Y. Feng, L. Bi, Z. Liu, D. Kong, Z. Yu, J. Catal. 290 (2012) 18-25.

[21] T.C. Wen, S.M. Lin, J.M. Tsai, J. Appl. Electrochem. 24 (1994) 233–238.

Table 1. Comparison of performances of some electrodes in electrocatalysis of methanol oxidation.

Electrode	E_{pa} /V	J/mA cm^{-2}	[Methanol]/M	Ref.
NiDMG/Ni[a]	0.65	15.9	0.10	[70]
NiPO-2/GCE[b]	0.66	1.70	1.00	[71]
Ni/AlLDH/NMCC[c]	0.78	31.8	1.20	[72]
Poly(Ni-curcumin)/GC	0.70	17.1	0.10	[73]
Ni/1,5-diaminonaphthalene/CPE	0.64	1.60	0.80	[64]
Ni/P(o-aminophenol)-SDS/CPE	0.65	16.7	0.37	[74]
$Ni_{80}Co_{20}$/PINA(SDS)/CPE	0.59	27.8	0.60	[55]
Pt/GC	0.80	1.90	0.50	[75]
Pt-C/GC	0.90	7.5	0.50	[75]
CPE/NiO NPs/SDS	0.80	20	0.40	Present work

[a] Nickel-dimethylglyoxime complex modified nickel electrode.

[b] Mesoporous nickel phosphate modified glassy carbon electrode.

[c] Ni/Al layered double hydroxide nanoparticle modified carbon ceramic electrode.

[22] C. Fan, D.L. Piron, A. Sleb, P. Paradis, J. Electrochem. Soc. 141 (1994) 382–387.
[23] I.A. Raj, K.I. Vasu, J. Appl. Electrochem. 20 (1990) 32-38.
[24] M.A. Casadei, D. Pletcher, Electrochim. Acta 33 (1988) 117–120.
[25] A.F.B. Barbosa, V.L. Oliveira, J. Drunen, G. Tremiliosi-Filho, J. Electroanal. Chem. 746 (2015) 31-38.
[26] T.R. Ling, K.T. Lien, J.J. Jow, T.Y. Lin, Electroanalysis 21 (2009) 2213-2219.
[27] Y.Y. Liao, T.C. Chou, Electroanalysis 12 (2000) 55-59.
[28] M.A. Abdel Rahim, R.M. Abdel Hameed, M.W. Khalil, J. Power Sources 134 (2004) 160–169.
[29] A.H. Touny, M.M. Saleh, Int. J. Electrochem. Sci. 13 (2018) 1042–1050.
[30] M. Asgari, M. Ghannadi Maragheh, R. Davarkhah, E. Lohrasbi, J. Electrochem. Soc. 158 (2011) K225-K229.
[31] M.G. Hosseini, M.M. Momeni, M. Faraji, Electroanalysis 22 (2010) 2620-2625.
[32] Y. Ma, L. Sheng, H. Zhao, K. Am, L. Yu, J. Xu, X. Zhao, Solid State Sci. 44 (2015) 49-55.
[33] M. Kundu, L. Liu, Mater. Lett. 144 (2015) 114-118.
[34] X. Qi, G. Su, G. Bo, L. Cao, W. Liu, Surf. Coat. Technol. 272 (2015) 79-85.
[35] M. Chiku, M. Toda, E. Higuchi, H. Inoue, J. Power Sources 286 (2015) 193-196.
[36] J. Zhao, Y. Tan, K. Su, J. Zhao, C. Yang, L. Sang, H. Lu, J.H. Chen, Appl. Surf. Sci. 337 (2015) 111-117.
[37] A.L. Gajengi, T. Sasaki, B.M. Bhanage, Catal. Commun. 72 (2015) 174-179.
[38] M. Tadic, D. Nikolic, Matjaz, G.R. Blake, J. Alloys Compd. 647 (2015) 1061-1068.
[39] R.A. Soomro, Z.H. Ibupoto, Sirajuddin, M. I. Abro, Sens. Actuators B 209 (2015) 966-974.
[40] A. Ahmadia, A. Nezamzadeh-Ejhieh, J. Electroanal. Chem. 801 (2017) 328–337.
[41] C.D. Gu, M.L. Huang, X. Ge, H. Zheng, X.L. Wang, J.P. Tu, Int. J. Hydrogen Energy 39 (2014) 10892-10901.
[42] N.A.M. Barakat, M.A. Abdelkareem, M.E. Newehy, H.Y. Kim, Nanoscale Res. Lett. 8 (2013) 402-407.
[43] N. Spinner, W.E. Mustain, Electrochim. Acta 56 (2011) 5656-5666.
[44] P. Wang, Y. Zhou, M. Hu, J. Chen, Appl. Surf. Sci. 392 (2017) 562-571.
[45] T.M. Mudrini, Z.D. Mojovi, A.Z. Ivanovi Šaši, N.S. Vukeli, Z.D. Upi, D.M. Jovanovi, Russ. J. Phys. Chem. A 87 (2013) 2127-2133.
[46] N.R. Stradiotto, K.E. Toghill, L. Xiao, A. Moshar, R.G. Compton, Electroanalysis 21 (2009) 2627-2633.
[47] R. Parsons, T. Vander Noot, J. Electroanal. Chem. 257 (1988) 9–45.
[48] K. Nishimura, K. Machida, M. Enyo, J. Electroanal. Chem. 251 (1988) 117–125.
[49] P.C. Biswas, Y. Nodasaka, M. Enyo, J. Appl. Electrochem. 26 (1996) 30–35.
[50] M. Jafarian, R.B. Moghaddam, M.G. Mahjani, F. Gobal, J. Appl. Electrochem. 36 (2006) 913–918.
[51] P.G. Westmoreland, R.A. Day, A. Underwood, Anal. Chem. 44 (1972) 737-740.
[52] R. Vittal, H. Gomathi, K.J. Kim, Adv. Colloid Interface Sci. 119 (2006) 55–68.
[53] M.J. Rosen. Surfactants and interfacial phenomena, New York, Wiley Interscience, 1978.
[54] P.A. Quintela, A.E. Kaifer, Langmuir 3 (1987) 769-773.
[55] B. Norouzi, M. Norouzi, J. Solid State Electrochem. 16 (2012) 3003–3010.
[56] B. Norouzi, M. Fatemi, J. Iran. Electrochem. Soc. 1 (2015) 9-15.
[57] O.K. Popoola, A.M. Elbagory, F. Ameer, A.A. Hussein, Molecules 18 (2013) 9049-9060.
[58] S. Iqbal, U. Younas, K.W. Chan, M. Zia-UI-Haq, M. Ismail, Molecules 17 (2012) 6020-6032.
[59] M. Mohadjerani, K. Pakzad, J. Appl. Chem. 7 (2013) 45-48.
[60] E. Ott, R.W. Cairns, Golden book of phase transitions, Wroclaw, 1 (2002) 1-123.
[61] S.D. Khairnar, M.R. Patil, V.S. Shrivastava, Iran. J. Catal. 8 (2018) 143-150.
[62] A. Nezamzadeh-Ejhieh, S. Tavakoli-Ghinani, C.R. Chim. 17 (2014) 49–61.
[63] M. Salavati-Niasari, F. Davar, M. Mazaheri, M. Shaterian, J. Magn. Magn. Mater. 320 (2008) 575-578.
[64] R. Ojani, J.B. Raoof, S.R. Hosseini, Electrochim. Acta 53 (2008) 2402-2407.
[65] A.J. Bard, L.R. Faulkner, Electrochemical methods, fundamentals and applications, Wiley, New York, USA, 2001.
[66] M.H. Sheikh-Mohseni, A. Nezamzadeh-Ejhieh, Electrochim. Acta 147 (2014) 572–581
[67] T.F. Connors, J.F. Rusling, A. Owlia, Anal. Chem. 57 (1985) 170–174.
[68] P.G. Westmoreland, R.A. Day, A. Underwood, Anal. Chem. 44 (1972) 737-740.
[69] C. Hu, S. Hu, Electrochim. Acta 49 (2004) 405-412.
[70] A. Nozad Golikand, M. Asgari, M. Ghannadi Maragheh, S. Shahrokhian, J. Electroanal. Chem. 588 (2006) 155-160.
[71] J. Yang, J. Tan, F. Yang, X. Li, X. Liu, D. Ma, Electrochem. Commun. 23 (2012) 13-16.
[72] G. Karim-nezhad, S. Pashazadeh, A. Pashazadeh, Chin. J. Catal. 33 (2012) 1809-1816.
[73] A. Ciszewski, G. Milczarek, B. Lewandowska, K. Krutowski, Electroanalysis 15 (2003) 518-523.
[74] R. Ojani, J.B. Raoof, S. Fathi, Electrochim. Acta 54 (2009) 2190-2196.
[75] A.V. Tripkovi, K.D. Popovi, J.D. Lovi, V.M. Jovanovi, A. Kowal, J. Electroanal. Chem. 572 (2004) 119-128.